

Piezoelectric ultrasonic motors: overview

Kenji Uchino

International Center for Actuators and Transducers, Intercollege Materials Research Laboratory, The Pennsylvania State University, University Park, PA 16802, USA

Received 26 July 1997, accepted for publication 20 October 1997

Abstract. This paper reviews recent developments of ultrasonic motors using piezoelectric resonant vibrations. Following the historical background, ultrasonic motors using standing and traveling waves are introduced. Driving principles and motor characteristics are explained in comparison with conventional electromagnetic motors. After a brief discussion on speed and thrust calculation, finally, reliability issues of ultrasonic motors are described.

1. Introduction

In office equipment such as printers and floppy disk drives, market research indicates that tiny motors smaller than 1 cm^3 would be in large demand over the next ten years. However, using the conventional electromagnetic motor structure, it is rather difficult to produce a motor with sufficient energy efficiency. Piezoelectric ultrasonic motors, whose efficiency is insensitive to size, are superior in the mm-size motor area.

In general, piezoelectric and electrostrictive actuators are classified into two categories, based on the type of driving voltage applied to the device and the nature of the strain induced by the voltage: (1) rigid displacement devices for which the strain is induced unidirectionally along an applied dc field, and (2) resonating displacement devices for which the alternating strain is excited by an ac field at the mechanical resonance frequency (ultrasonic motors). The first category can be further divided into two types: servo displacement transducers (positioners) controlled by a feedback system through a position-detection signal, and pulse-drive motors operated in a simple on/off switching mode, exemplified by dot-matrix printers.

The AC resonant displacement is not directly proportional to the applied voltage, but is, instead, dependent on adjustment of the drive frequency. Although the positioning accuracy is not as high as that of the rigid displacement devices, very high speed motion due to the high frequency is an attractive feature of the ultrasonic motors. Servo displacement transducers, which use feedback voltage superimposed on the DC bias, are used as positioners for optical and precision machinery systems. In contrast, a pulse drive motor generates only on/off strains, suitable for the impact elements of dot-matrix or ink-jet printers.

The materials requirements for these classes of devices are somewhat different, and certain compounds will be

better suited for particular applications. The ultrasonic motor, for instance, requires a very hard piezoelectric with a high mechanical quality factor Q , in order to minimize heat generation and maximize displacement. Note that the resonance displacement is equal to αdEL , where d is a piezoelectric constant, E , applied electric field, L , sample length and α is an amplification factor proportional to the mechanical Q . The servo-displacement transducer suffers most from strain hysteresis and, therefore, a PMN electrostrictor is preferred for this application. Notice that even in a feedback system the hysteresis results in a much lower response speed. The pulse-drive motor requires a low-permittivity material aiming at quick response with a limited power supply rather than a small hysteresis, so that soft PZT piezoelectrics are preferred to the high-permittivity PMN for this application.

This paper deals with ultrasonic motors using resonant vibrations. Following the historical background, various ultrasonic motors are introduced. Driving principles and motor characteristics are explained in comparison with the conventional electromagnetic motors. After a brief discussion on speed and thrust calculation, finally, reliability issues of ultrasonic motors are described.

2. Classification of ultrasonic motors

2.1. Historical background

Electromagnetic motors were invented more than a hundred years ago. While these motors still dominate the industry, a drastic improvement cannot be expected except through new discoveries in magnetic or superconducting materials. Regarding conventional electromagnetic motors, tiny motors smaller than 1 cm^3 are rather difficult to produce with sufficient energy efficiency. Therefore, a new class of motors using high power ultrasonic energy—ultrasonic motors—is gaining widespread attention. Ultrasonic motors made with piezoceramics whose efficiency is insensitive to

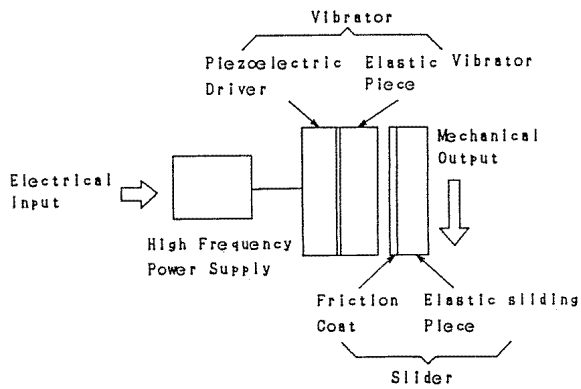


Figure 1. Fundamental construction of ultrasonic motors.

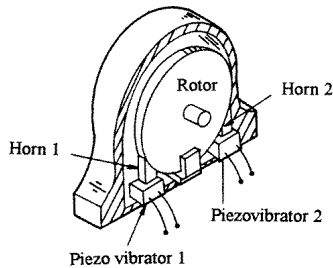


Figure 2. Ultrasonic motor by Barth.

size are superior in the mini-motor area. Figure 1 shows the basic construction of ultrasonic motors, which consist of a high-frequency power supply, a vibrator and a slider. Further, the vibrator is composed of a piezoelectric driving component and an elastic vibratory part, and the slider is composed of an elastic moving part and a friction coat.

Though there had been some earlier attempts, the practical ultrasonic motor was proposed firstly by H V Barth of IBM in 1973 [1]. As shown in figure 2, the rotor was pressed against two horns placed at different locations. By exciting one of the horns, the rotor was driven in one direction, and by exciting the other horn, the rotation direction was reversed. Various mechanisms based on virtually the same principle were proposed by V V Lavrinenko *et al* [2] and P E Vasiliev *et al* [3] in the former USSR. Because of difficulty in maintaining a constant vibration amplitude with temperature rise, wear and tear, the motors were not of much practical use at that time.

In the 1980s, with increasing chip pattern density, the semiconductor industry began to request much more precise and sophisticated positioners which do not generate magnetic field noise. This urgent request has accelerated the developments in ultrasonic motors. Another advantage of ultrasonic motors over the conventional electromagnetic motors with expensive copper coils, is the improved availability of piezoelectric ceramics at reasonable cost. Japanese manufacturers are producing piezoelectric buzzers around the 30–40 cent price range at the moment.

Let us summarize the merits and demerits of the ultrasonic motors.

Merits.

- (1) Low speed and high torque—direct drive.
 - (2) Quick response, wide velocity range, hard brake and no backlash: excellent controllability; fine position resolution.
 - (3) High power/weight ratio and high efficiency.
 - (4) Quiet drive.
 - (5) Compact size and light weight.
 - (6) Simple structure and easy production process.
 - (7) Negligible effect from external magnetic or radioactive fields, and also no generation of these fields.
- #### Demerits.
- (8) Necessity for a high frequency power supply.
 - (9) Less durability due to frictional drive.
 - (10) Drooping torque–speed characteristics.

2.2. Classification and principles of ultrasonic motors

From a customer's point of view, there are rotary and linear type motors. If we categorize them from the vibrator shape, there are rod type, π -shaped, ring (square) and cylinder types, which are illustrated in figure 3. Two categories are being investigated for ultrasonic motors from a vibration characteristic viewpoint: a standing-wave type and a propagating-wave type. Refresh your memory on the wave formulas. The standing wave is expressed by

$$u_s(x, t) = A \cos kx \cos \omega t \quad (1)$$

while the propagating wave is expressed as

$$u_p(x, t) = A \cos(kx - \omega t). \quad (2)$$

Using a trigonometric relation, (2) can be transformed as

$$u_p(x, t) = A \cos kx \cos \omega t + A \cos(kx - \pi/2) \cos(\omega t - \pi/2). \quad (3)$$

This leads to an important result, i.e. a propagating wave can be generated by superimposing two standing waves whose phases differ by 90° from each other both in time and in space. This principle is necessary to generate a propagating wave on a limited volume/size substance, because only standing waves can be excited stably in a finite size.

2.2.1. Standing-wave type. The standing-wave type is sometimes referred to as a vibratory-coupler type or a 'woodpecker' type, where a vibratory piece is connected to a piezoelectric driver and the tip portion generates flat-elliptical movement. Figure 4 shows a simple model proposed by T Sashida [4]. A vibratory piece is attached to a rotor or a slider with a slight cant angle θ . Take the x - y coordinate so that the x axis is normal to the rotor face. When a vibration displacement

$$u_x = u_0 \sin(\omega t + \alpha) \quad (4)$$

is excited at the piezoelectric vibrator, the vibratory piece generates bending because of restriction by the rotor, so that the tip moves along the rotor face between $A \rightarrow B$, and freely between $B \rightarrow A$. If the vibratory piece and the

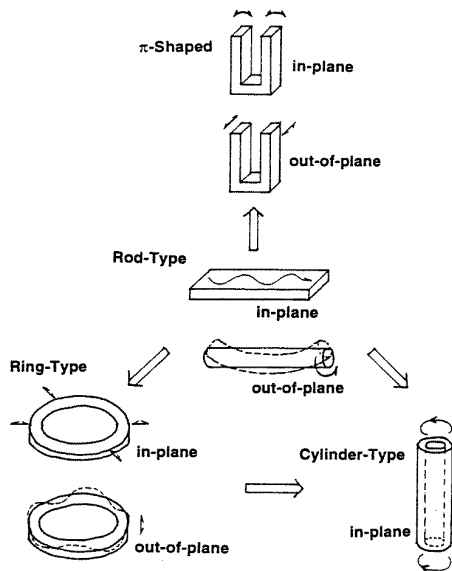


Figure 3. Vibrator shapes for ultrasonic motors.

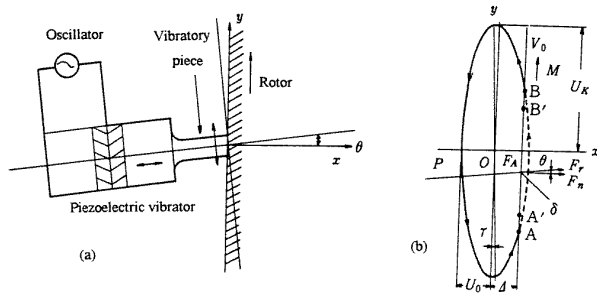


Figure 4. Vibratory coupler type motor (a) and its tip locus (b).

piezo-vibrator are tuned properly, they form a resonating structure, and if the bending deformation is sufficiently small compared with the piece length, the tip locus during the free vibration ($B \rightarrow A$) is represented by

$$\begin{aligned} x &= u_0 \sin(\omega t + \alpha) \\ y &= u_1 \sin(\omega t + \beta) \end{aligned} \quad (5)$$

which is an elliptical locus. Therefore, only the duration $A \rightarrow B$ provides a unidirectional force to the rotor through friction, i.e. intermittent rotational torque or thrust. However, because of the inertia of the rotor, the rotation speed ripple is not large to observe. The standing-wave type, in general, is low in cost (one vibration source) and has high efficiency (up to 98% theoretically), but lack of control in both clockwise and counterclockwise directions is a problem.

2.2.2. Propagating-wave type. By comparison, the propagating-wave type (a surface-wave or 'surfing' type) combines two standing waves with a 90 degree phase difference both in time and in space. The principle is shown in figure 5. A surface particle of the elastic body draws an elliptical locus due to the coupling of longitudinal

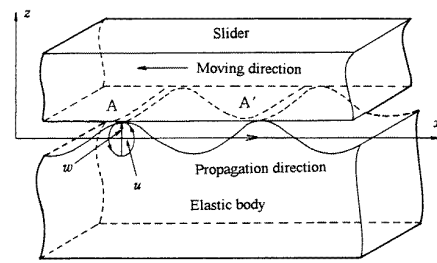


Figure 5. Principle of the propagating-wave type motor.

and transverse waves. This type requires, in general, two vibration sources to generate one propagating wave, leading to low efficiency (not more than 50%), but it is controllable in both the rotational directions.

3. Standing-wave type motors

3.1. Rotary motors

T Sashida developed a rotary type motor similar to the fundamental structure [4]. Four vibratory pieces were installed on the edge face of a cylindrical vibrator, and pressed onto the rotor. This is one of the prototypes which triggered the present development fever on ultrasonic motors. A rotation speed of 1500 rpm, torque of 0.08 N m and output of 12 W (efficiency 40%) were obtained under an input of 30 W at 35 kHz. This type of ultrasonic motor can provide a speed much higher than the inchworm types, because of high frequency and an amplified vibration displacement at the resonance frequency.

Hitachi Maxel significantly improved the torque and efficiency by using a torsional coupler replacing Sashida's vibratory pieces (figure 6), and by increasing the pressing force with a bolt [5]. The torsional coupler looks like an old fashioned TV channel knob, consisting of two legs which transform longitudinal vibration generated by the Langevin vibrator to a bending mode of the knob disk, and a vibratory extruder. Notice that this extruder is aligned with a certain cant angle to the legs, which transforms the bending to a torsion vibration. This transverse moment coupled with the bending up-down motion leads to an elliptical rotation on the tip portion, as illustrated in figure 6(b). The optimum pressing force to obtain the maximum thrust is obtained, when the ellipse locus is deformed roughly by half. A motor 30 mm × 60 mm in size and 20–30° in cant angle between a leg and a vibratory piece provided torque as high as 1.3 N m and the efficiency of 80%. However, this type provides only unidirectional rotation. Notice that even though the drive of the motor is intermittent, the output rotation becomes very smooth because of the inertia of the rotor.

The Penn State University has developed a compact ultrasonic rotary motor as tiny as 3 mm in diameter. As shown in figure 7, the stator consists of a piezoelectric ring and two concave/convex metal endcaps with 'windmill' shaped slots bonded together, so as to generate a coupled vibration of up-down and torsional type [6]. Since the component number and the fabrication process were

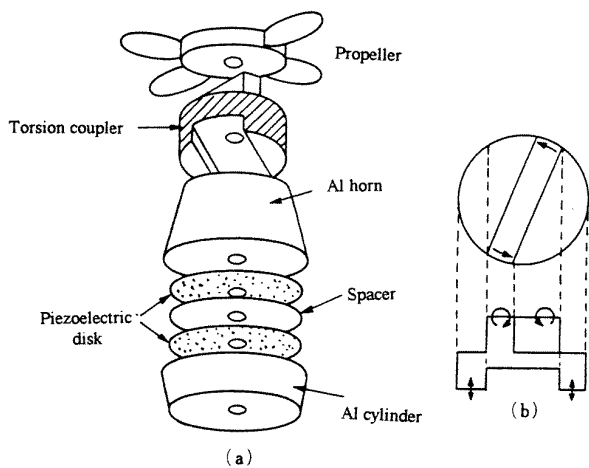


Figure 6. Torsional coupler ultrasonic motor (a) and the motion of the torsional coupler (b).

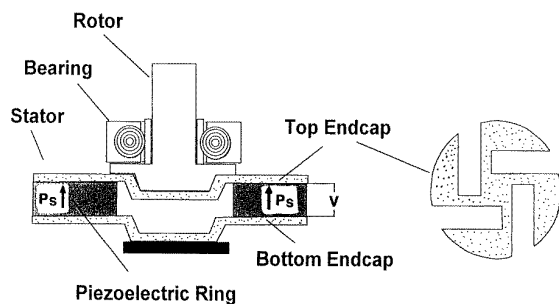


Figure 7. 'Windmill' motor with a disk-shaped torsional coupler.

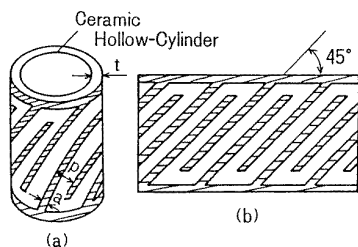


Figure 8. Piezoelectric cylinder torsional vibrator (a) and the electrode pattern (b).

minimized, the fabrication price would be decreased remarkably, and it would be adaptive to disposable usage. When driven at 160 kHz, the maximum revolution 600 rpm and the maximum torque 1 mN m were obtained for a 11 mm diameter motor.

Tokin developed a piezoelectric ceramic cylinder for a torsional vibrator (figure 8) [7]. Using an interdigital type electrode pattern printed with 45° cant angle on the cylinder surface, torsion vibration was generated, which is applicable to a simple ultrasonic motor.

S Ueha *et al* proposed a two-vibration-mode coupled type (figure 9), i.e. a torsional Langevin vibrator was combined with three multilayer actuators to generate larger longitudinal and transverse surface displacement of the stator, as well as to control their phase difference [8]. The

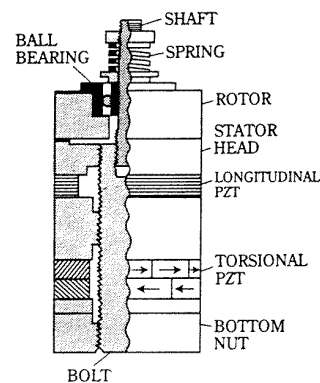


Figure 9. Two-vibration-mode coupled type motor.

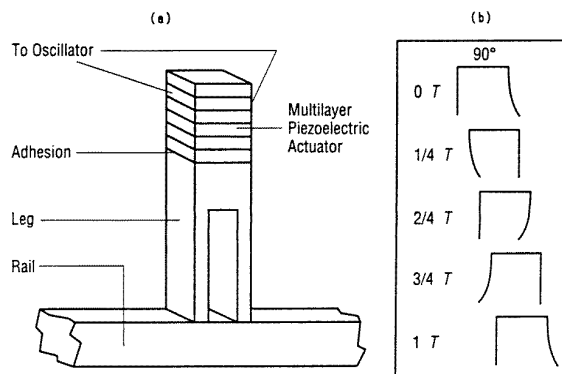


Figure 10. π -shaped linear ultrasonic motor: (a) construction and (b) walking principle. Note the 90 degree phase difference like a human walk.

phase change can change the rotation direction.

3.2. Linear motors

K Uchino *et al* invented a π -shaped linear motor [9]. This linear motor is equipped with a multilayer piezoelectric actuator and fork-shaped metallic legs as shown in figure 10. Since there is a slight difference in the mechanical resonance frequency between the two legs, the phase difference between the bending vibrations of both legs can be controlled by changing the drive frequency. The walking slider moves in a way similar to a horse using its fore and hind legs when trotting. A test motor $20 \times 20 \times 5 \text{ mm}^3$ in dimension exhibited a maximum speed of 20 cm s^{-1} and a maximum thrust of 0.2 kgf with a maximum efficiency of 20%, when driven at 98 kHz at 6 V (actual power = 0.7 W). Figure 11 shows the motor characteristics of the linear motor. This motor has been employed in a precision X-Y stage.

Tomikawa's rectangular plate motor is also intriguing [10]. As shown in figure 12, a combination of the two modes forms an elliptical displacement motion. The two modes chosen were the first longitudinal mode (L_1 mode) and the eighth bending mode (B_8), whose resonance frequencies were almost the same. By applying voltages with a phase difference of 90° to the L-mode and B-mode drive electrodes, elliptical motion in the same direction can

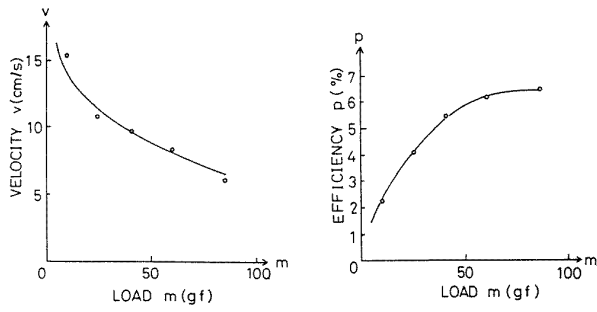


Figure 11. Motor characteristics of the π -shaped motor.

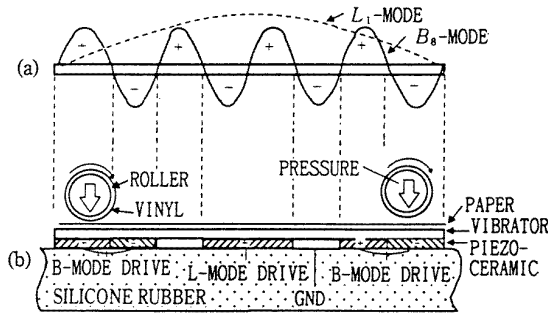


Figure 12. L_1 and B_8 double-mode vibrator motor.

be obtained at both ends of this plate, leading to rotation of the rollers in contact with these points. Anticipated applications are paper or card senders. The reader can find other linear motor ideas in Ueha and Tomikawa's book [11].

4. Propagating wave type motors

4.1. Linear motors

T Sashida and S Ueha *et al* manufactured a linear motor as illustrated in figure 13 [12, 13]. The two piezoelectric vibrators installed at both ends of a transmittance steel rod excite and receive the traveling transverse wave (antisymmetric fundamental Lamb wave mode). Adjusting a load resistance in the receiving vibrator leads to a perfect traveling wave. Exchanging the role of exciting and receiving piezo-components provided a reverse moving direction.

The bending vibration transmitting via the rail rod is represented by the following differential equation:

$$(\partial^2 w(x, t) / \partial t^2) + (EI / \rho A)(\partial^4 w(x, t) / \partial x^4) = 0 \quad (6)$$

where $w(x, t)$ is a transverse displacement (see figure 5), x , the coordinate along the rod axis, E , Young's modulus of the rod, A , the cross sectional area, ρ , density and I is the moment of inertia of the cross-section. Assuming a general solution of (6) as

$$w(x, t) = W(x)(A \sin \omega t + B \cos \omega t) \quad (7)$$

the wave transmission velocity v and wavelength λ are calculated as

$$v = (EI / \rho A)^{1/4} \sqrt{\omega} \quad (8)$$

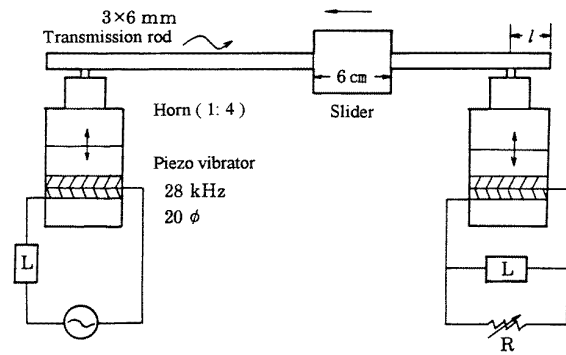


Figure 13. Linear motor using a bending vibration.

$$\lambda = 2\pi(EI / \rho A)^{1/4} / \sqrt{\omega}. \quad (9)$$

Using the bending vibration, the wavelength λ can be easily chosen as short as several mm to satisfy a stable surface contact with the slider by changing the cross section area A or the moment of inertia I of the transmission rod. In the case of figure 13, $\lambda = 26.8$ mm.

A slider, the contact face of which is coated with rubber or vinyl resin sheet, clamps the transmission rod with an appropriate force. The transmission efficiency is strongly affected by the vibration source position on the rod, showing a periodic change with the distance from the free end of the rod to the position of the vibrator. Taking account of the wave phase, the vibration source should be fixed at the distance of the wavelength λ (i.e. 26.8 mm) from the rod end.

The slider made of a steel clasper 60 mm in length, which theoretically covers two waves, was driven at a speed of 20 cm s^{-1} with a thrust of 50 N at 28 kHz. A serious problem with this type is found in low efficiency around 3% because the whole rod must be excited even when only a small portion is utilized for the output. Thus, ring type motors were invented by Sashida, where the whole rod can be utilized, because the lengths of the stator and rotor are the same.

4.2. Rotary motors

When we deform the rod discussed in the previous section to make a ring by connecting the two ends topologically, we can make a rotary type motor using a bending vibration. Two types of 'ring' motor design are possible: (a) bending mode and (b) extensional mode [14]. Though the principle is similar to the linear type, more sophisticated structures are employed in the ceramic poling and in the mechanical support mechanism.

4.2.1. Principle of 'surfing' rotary motors. In general, when a vibration source is driven at one position on a closed ring (circular or square) at a frequency corresponding to the resonance of this ring, only a standing wave is excited, because the vibration propagates in two directions symmetrically to the vibration source and these interfere with each other. When multiple vibration sources are installed on the ring, displacements can be obtained

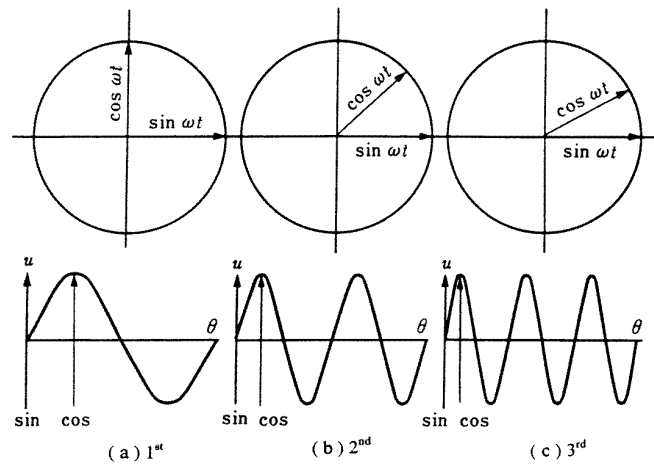


Figure 14. Vibration source positions for generating a propagating wave in a ring.

by superimposing all the waves (two waves from each vibration source). Using this superposition principle, we can generate a propagating wave which is a rotation of the standing-wave shape, even in a closed ring.

Assuming a vibration source of $A \cos \omega t$ at the point $\theta = 0$ of the elastic ring, the n th mode standing wave can be expressed by

$$u(\theta, t) = A \cos n\theta \cos \omega t \quad (10)$$

and the traveling wave by

$$u(\theta, t) = A \cos(n\theta - \omega t). \quad (11)$$

Since the traveling wave can be expressed as a superimposition of two standing waves as

$$u(\theta, t) = A \cos n\theta \cos \omega t + A \cos(n\theta - \pi/2) \cos(\omega t - \pi/2) \quad (12)$$

we derive an important principle: a propagating wave can be generated by superimposing two standing waves whose phases differ by 90° from each other both in time and in space. More generally, the phase difference can be chosen arbitrarily (except $0, -\pi, \pi$), as long as the phase difference is the same in space and in time. The vibration source positions for generating a propagating wave on a ring are illustrated in figure 14. In principle, the excitation at only two parts of the ring is sufficient to generate a traveling wave. However, in practice, the number of the vibration sources is increased to as many as possible to increase the mechanical output. The symmetry of the electrode structure needs to be considered.

4.2.2. Examples of ‘surfing’ rotary motors. Figure 15 shows the famous Sashida motor [15]. By means of the traveling elastic wave induced by a thin piezoelectric ring, a ring-type slider in contact with the ‘rippled’ surface of the elastic body bonded onto the piezoelectric is driven in both directions by exchanging the sine and cosine voltage inputs. Another advantage is its thin design, which makes it suitable for installation in cameras as an automatic focusing

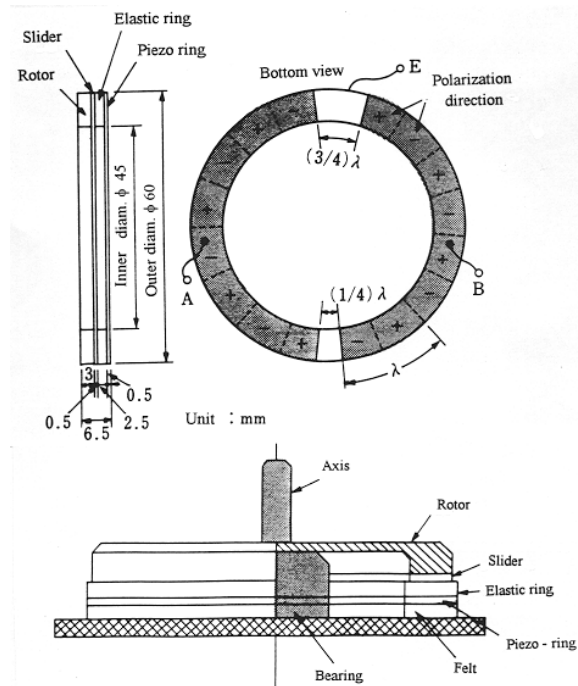


Figure 15. Stator structure of Sashida's motor.

device. Eighty percent of the exchange lenses in Canon's ‘EOS’ camera series have already been replaced by the ultrasonic motor mechanism. Most of the studies on ultrasonic motors done in the US and Japan have been modifications of Sashida's type.

The PZT piezoelectric ring is divided into 16 positively and negatively poled regions and two asymmetric electrode gap regions so as to generate a ninth mode propagating wave at 44 kHz. A proto-type was composed of a brass ring of 60 mm in outer diameter, 45 mm in inner diameter and 2.5 mm in thickness, bonded onto a PZT ceramic ring of 0.5 mm in thickness with divided electrodes on the back-side. The rotor was made of polymer coated with hard rubber or polyurethane. Figure 16 shows Sashida's motor

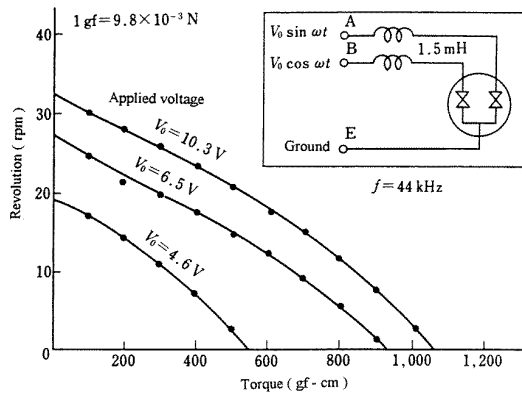


Figure 16. Motor characteristics of Sashida's motor.

characteristics.

Canon utilized the 'surfing' motor for a camera automatic focusing mechanism, installing the ring motor compactly in the lens frame. It is noteworthy that the stator elastic ring has many teeth, which can magnify the transverse elliptical displacement and improve the speed. The lens position can be shifted back and forth through a screw mechanism. The advantages of this motor over the conventional electromagnetic motor are:

- (1) Silent drive due to the ultrasonic frequency drive and no gear mechanism (i.e. more suitable to video cameras with microphones).
- (2) Thin motor design and no speed reduction mechanism such as gears, leading to space saving.
- (3) Energy saving.

A general problem encountered in these traveling wave type motors is the support of the stator. In the case of a standing wave motor, the nodal points or lines are generally supported; this causes minimum effects on the resonance vibration. In contrast, a traveling wave does not have such steady nodal points or lines. Thus, special considerations are necessary. In figure 15, the stator is basically fixed very gently along the axial direction through felt so as not to suppress the bending vibration. It is important to note that the stop pins which latch onto the stator teeth only provide high rigidity against the rotation.

Matsushita Electric proposed a nodal line support method using a higher order vibration mode (see figure 17(b)) [16]. Figure 17(a) shows the stator structure, where a wide ring was supported at the nodal circular line and 'teeth' were arranged on the maximum amplitude circle to obtain larger revolution.

Seiko Instruments miniaturized the ultrasonic motor to as tiny as 10 mm in diameter using basically the same principle [17]. Figure 18 shows the construction of this small motor with 10 mm diameter and 4.5 mm thickness. A driving voltage of 3 V and a current 60 mA provides 6000 rev min⁻¹ (no load) with torque of 0.1 mN m. AlliedSignal developed ultrasonic motors similar to Shinsei's, which would be utilized as mechanical switches for launching missiles [18].

It is important to note that the unimorph (bonded type of a piezoceramic plate and a metal plate) bending actuation

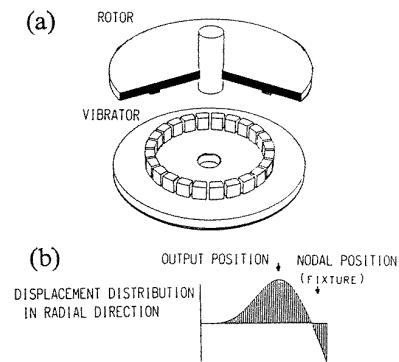


Figure 17. (a) Tooth shaped stator and (b) a higher order vibration mode with a nodal line for fixing.

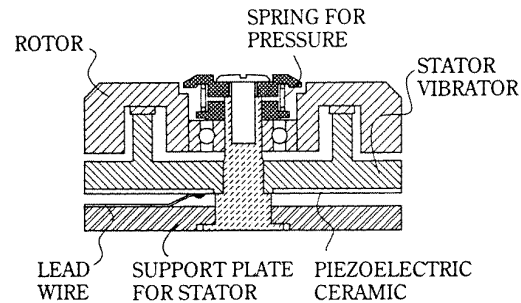


Figure 18. Construction of Seiko's motor.

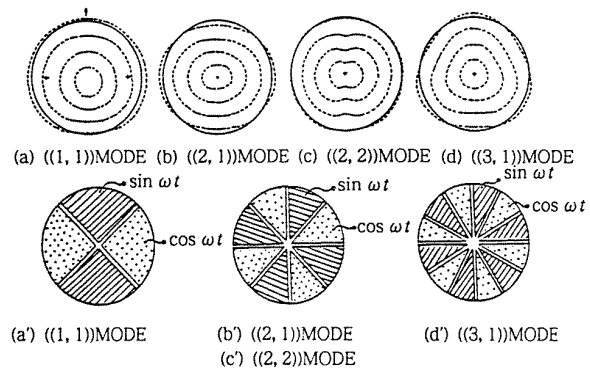


Figure 19. Disk type hula-hoop motor.

can not provide high efficiency theoretically, because the electromechanical coupling factor k is usually less than 10%. Therefore, instead of the unimorph structure, a simple disk was directly used to make motors [19, 20]. Figure 19 shows (1,1), (2,1) and (3,1) modes of a simple disk, which are axial-asymmetric modes. Both the inner and outer circumferences can provide a rotation like a 'hula hoop'.

Another intriguing design is a 'plate-spinning' type proposed by Tokin [21]. Figure 20 shows its principle. A rotary bending vibration was excited on a PZT rod by a combination of sine and cosine voltages, then a cup was made to contact the 'spinning' rod with the internal face for achieving rotation.

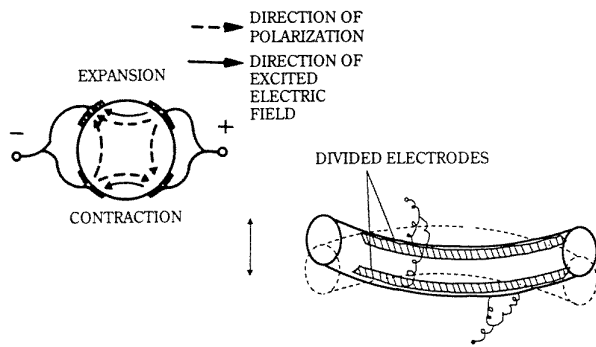


Figure 20. 'Plate-spinning' type motor by Tokin.

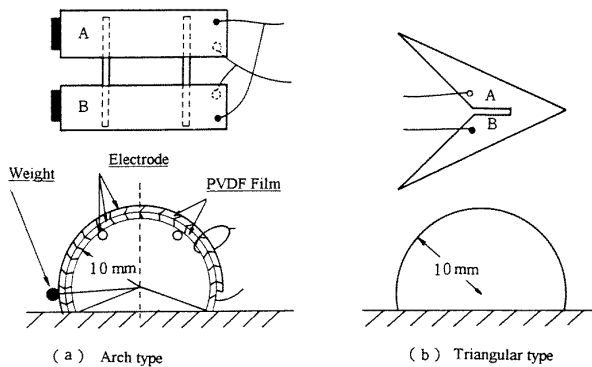


Figure 21. PVDF walking mechanism.

4.3. Comparison among various ultrasonic motors

The standing-wave type, in general, is low in cost (one vibration source) and has high efficiency (up to 98% theoretically), but lack of control in both clockwise and counterclockwise directions is a problem. By comparison, the propagating-wave type combines two standing waves with a 90 degree phase difference both in time and in space. This type requires, in general, two vibration sources to generate one propagating wave, leading to low efficiency (not more than 50%), but is controllable in both rotational directions.

Table 1 summarizes the motor characteristics of the vibration coupler standing wave type (Hitachi Maxel), surface propagating wave type (Shinsei Industry) and a compromised 'teeth' vibrator type (Matsushita) [22].

5. Micro-walking machines

Recent biomedical experiments and medical surgery require sophisticated tiny actuators for micro-manipulation of optical fibers, catheters, micro-surgery knives etc. Thus, microactuators, particularly micro-walking devices, have been studied intensively.

The first systematic study was performed by T Hayashi on PVDF bimorph actuators [23]. Figure 21 shows two designs of micro-machines. The devices were fabricated using two 30 μm thick PVDF films bonded together with a curvature of 1 cm^{-1} . The curved bimorph is electrically

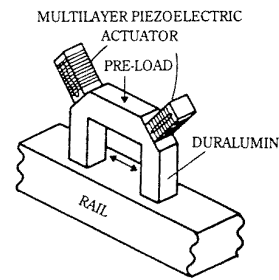


Figure 22. π -shaped ultrasonic linear motor.

driven at the mechanical resonance, which generates a large opening and closing motion at the contact point with the floor. In order to control the device in both clockwise and counter-clockwise rotations, a slight difference of the leg width between the right and left legs was intentionally made, so as to provide a slight difference between their resonance frequencies. By choosing a suitable drive frequency, the right or left leg pair is more mechanically excited, leading to curving.

The π -shape ultrasonic motor described in section 3.2 can be modified to be driven in a propagating wave manner. K Ohnishi *et al* developed a motor as shown in figure 22, where two multilayer actuators were installed at the two corners of the π -shaped frame, and driven with a 90 degree phase difference, revealing a 'trotting' leg motion [24].

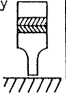
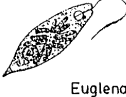
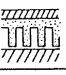



One ceramic multilayer component actuator was proposed by Mitsui Sekka [25]. Figure 23 shows the electrode pattern. Only by the external connection, a combined vibration of the longitudinal L_1 and bending B_2 modes could be excited. The motor characteristics are shown in figure 24.

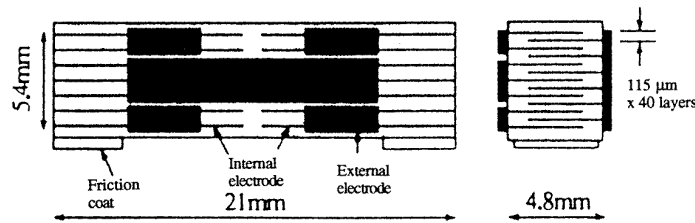
Let us introduce a surface acoustic wave motor proposed by Kurosawa and Higuchi [26]. As shown in figure 25(a), Rayleigh waves were excited in two crossed directions on a 127.8° rotation Y-LiNbO_3 plate with two pairs of interdigital electrode patterns. Figure 25(b) shows a slider structure with three balls as legs. The driving vibration amplitude and the wave velocity of the Rayleigh waves were adjusted to 6.1 nm and 22 cm s^{-1} for both x and y directions. It is important to note that even though the up-down vibrational amplitude is much smaller ($<1/10$) than the surface roughness of the LiNbO_3 , the slider was transferred smoothly. The mechanism has not been clarified yet; it might be due to the locally enhanced friction force through a ball-point contact. This may be categorized as a nano-actuator.

6. Speed/thrust calculation

We will introduce the speed and thrust calculation for ultrasonic motors roughly in this section [27]. These calculations depend on the type of motor as well as the contact conditions. The intermittent drive must be considered for the vibratory coupler type motors, while the surface wave type provides the continuous drive in the calculation. The contact models include:

Table 1. Comparison of the motor characteristics of the vibration coupler standing wave type (Hitachi Maxel), surface propagating wave type (Shinsei Industry) and a compromised 'teeth' vibrator type (Matsushita).

CHARACTERISTICS TYPES	Rotation	Rotation Speed [rpm]	Rotation Torque [kgf·cm]	Efficiency [%]	Size	Analogy
Vibratory Coupler Type 	Uni- Direction	600	13	80	Slim & Long	 Euglena
Compromise Type 	Reversible	600	1	45	⋮ ⋮ ⋮	 Paramecium
Surface Wave Type 	Reversible	600	0.5	30	Wide & Thin	 Amoeba

**Figure 23.** Multilayer ceramic simple linear motor.

- (1) rigid slider and rigid stator,
- (2) compliant slider and rigid stator,
- (3) compliant slider and compliant stator.

6.1. Surface wave type

If the rigid slider and rigid stator model is employed, the slider speed can be obtained from the horizontal velocity of the surface portion of the stator (see figure 26). If the frequency and wavelength of the stator vibration are f and λ , respectively, and the normal vibration amplitude (up-down) is Z , and the distance between the surface and the neutral plane is e_0 , the wave propagation speed is given by

$$V = f\lambda. \quad (13)$$

This is the sound phase velocity of the vibration mode! In contrast, the speed of the slider is given by

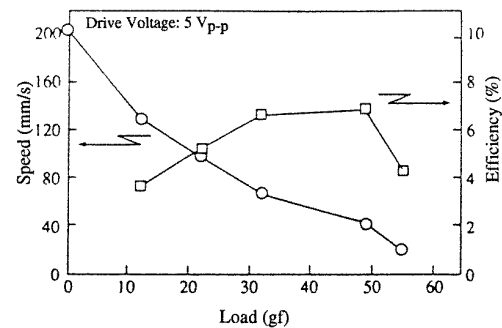
$$v = 4\pi^2 Z e_0 f / \lambda. \quad (14)$$

It is noteworthy that the slider moves in the opposite direction with respect to the wave traveling direction.

6.2. Vibration coupler type

Here, the compliant slider—rigid stator model is introduced. As shown in figure 27, the horizontal and vertical displacements of the rigid stator are given by

$$\begin{aligned} a &= a_0 \cos \omega t \\ b &= b_0 \sin \omega t. \end{aligned} \quad (15)$$

**Figure 24.** Motor characteristics of the Mitsui Sekka motor.

Thus, the horizontal velocity becomes

$$v_h = (\partial a / \partial t) = -a_0 \omega \sin \omega t. \quad (16)$$

We usually employ the following three hypotheses for further calculations:

Hypothesis 1. Normal force is given as follows, using a characteristic angle ϕ (between P_1 and P_2):

$$\begin{aligned} n &= \beta [\sin \omega t - \cos(\phi/2)] \\ &\text{for } (\pi/2 - \phi/2) < \omega t < (\pi/2 + \phi/2) \text{ (in contact)} \\ n &= 0 \quad \text{for } 0 < \omega t < (\pi/2 - \phi/2), (\pi/2 + \phi/2) \\ &\quad < \omega t < 2\pi \text{ (out of contact).} \end{aligned} \quad (17)$$

Hypothesis 2. The slider speed is constant (V_0).

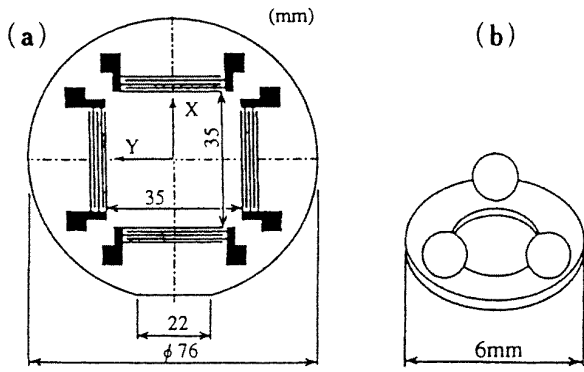


Figure 25. (a) Stator structure of the surface acoustic wave motor. (b) Slider structure of the SAW motor.

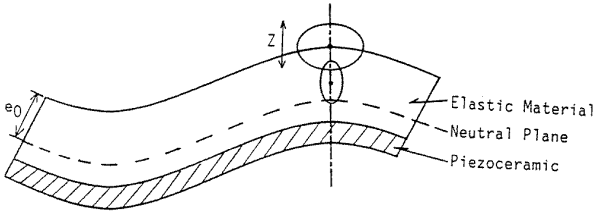


Figure 26. Displacement configuration of the stator of the surface wave type motor.

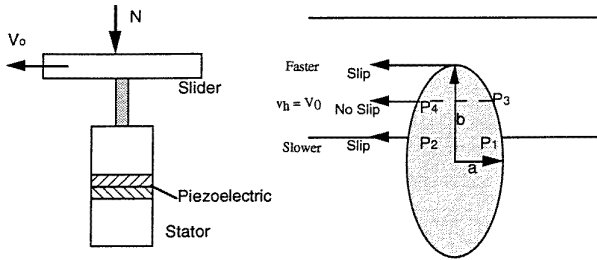


Figure 27. Compliant slider and rigid stator model.

Hypothesis 3. The maximum thrust is given by the dynamic friction constant μ_d :

$$\begin{aligned}
 f &= -\mu_d n && \text{accelerating force for } (\pi/2 - \psi/2) \\
 &< \omega t < (\pi/2 + \psi/2) \\
 f &= \mu_d n && \text{dragging force for } (\pi/2 - \phi/2) \\
 &< \omega t < (\pi/2 - \psi/2), (\pi/2 + \psi/2) < \omega t \\
 &< (\pi/2 + \phi/2).
 \end{aligned}
 \tag{18}$$

The main results are summarized. If we know ϕ experimentally (or theoretically taking into account the geometry and elasticity) under a certain normal force N , we can calculate the no-load speed V_0 from

$$V_0 = -a_0 \omega \sin(\phi/2) / (\phi/2)
 \tag{19}$$

and no-slip position angle ψ from the following relation:

$$\cos(\psi/2) = \sin(\phi/2) / (\phi/2).
 \tag{20}$$

Then, finally, we can obtain the thrust from

$$\begin{aligned}
 F &= \mu_d N \{ 1 - 2[\sin(\psi/2) - (\psi/2) \cos(\phi/2)] / [\sin(\phi/2) \\
 &\quad - (\phi/2) \cos(\phi/2)] \}.
 \end{aligned}
 \tag{21}$$

In the case of $\phi = 0$, $\psi = 0$, $V_0 = -a_0 \omega$, $F = -0.155 \mu_d N$; while in the case of $\phi = \pi$, $\cos(\psi/2) = 2/\pi$, $V_0 = -(2/\pi) a_0 \omega$ and $F = -0.542 \mu_d N$. With increasing contact period of the vibratory piece, the thrust F increases by sacrificing the speed.

For other model calculations, refer to the book [11].

7. Reliability of ultrasonic motors

In the development of ultrasonic motors, the following themes should be systematically studied:

- (1) Measuring methods for high-field electromechanical couplings.
- (2) Materials development (low loss and high vibration velocity).
- (3) Piezo-actuator designs.
 - (a) Heat generation mechanism.
 - (b) Degradation mechanisms.
 - (c) New multilayer actuator designs.
- (4) USM designs.
 - (a) Displacement magnification mechanisms (horn, hinge-lever).
 - (b) USM types (standing-wave type, propagating-wave type).
 - (c) Frictional contact part.
- (5) Drive/control.
 - (a) High frequency/high power supply.
 - (b) Resonance/antiresonance usage.

We will discuss the reliability issues in this section: heat generation, friction materials and drive/control techniques in the ultrasonic motors.

7.1. Heat generation

The largest problem in ultrasonic motors is heat generation, which sometimes drives temperatures up to 120 °C and causes a serious degradation of the motor characteristics through depoling of the piezoceramic. Therefore, the ultrasonic motor requires a very hard type piezoelectric with a high mechanical quality factor Q , leading to the suppression of heat generation. It is also notable that the actual mechanical vibration amplitude at the resonance frequency is directly proportional to this Q value.

Figure 28 shows mechanical Q versus basic composition x at effective vibration velocity $v_0 = 0.05 \text{ m s}^{-1}$ and 0.5 m s^{-1} for $\text{Pb}(\text{Zr}_x\text{Ti}_{1-x})\text{O}_3$ doped with 2.1 at.% of Fe [28]. The decrease in mechanical Q with an increase of vibration level is minimum around the rhombohedral-tetragonal morphotropic phase boundary (52/48). In other words, the worst material at a small vibration level becomes the best at a large vibration level, and the data obtained by a conventional impedance analyser are not relevant to high power materials.

Figure 29 shows an important notion on heat generation from the piezoelectric material. The resistances R_d and

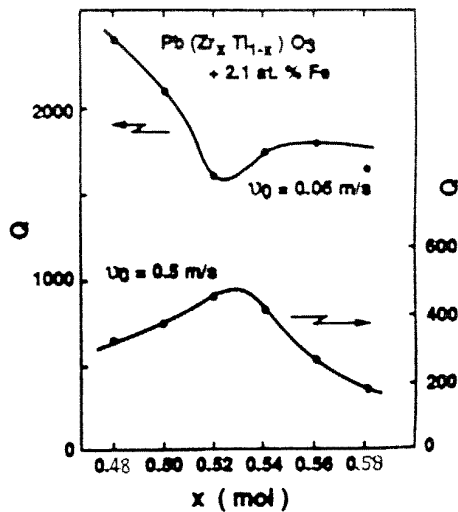


Figure 28. Mechanical quality factor Q against basic composition x at vibration velocity $v_0 = 0.05$ and 0.5 m s^{-1} for $\text{Pb}(\text{Zr}_x\text{Ti}_{1-x})\text{O}_3 + 2.1 \text{ at.} \% \text{ Fe}$ ceramics.

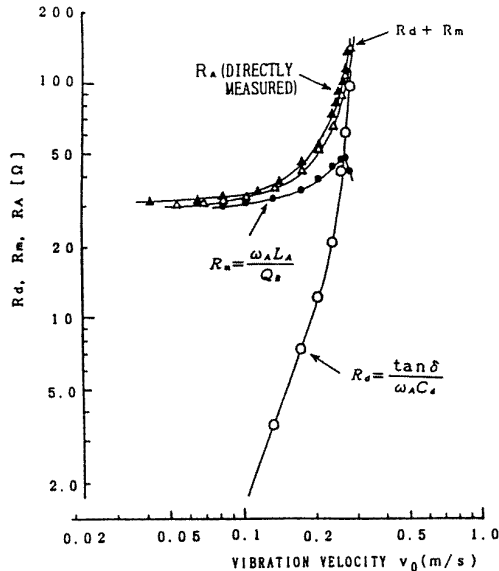


Figure 29. Vibration velocity dependence of the resistances R_d and R_m in the equivalent electrical circuit.

R_m in the equivalent electrical circuit are separately plotted as a function of vibration velocity [29]. Note that R_m , mainly related to the mechanical loss, is insensitive to the vibration velocity, while R_d , related to the dielectric loss, changes significantly around a certain critical vibration velocity. Thus, the resonance loss at a small vibration velocity is mainly determined by the mechanical loss, and with increasing vibration velocity, the dielectric loss contribution significantly increases. We can conclude that heat generation is caused by dielectric loss (i.e. P - E hysteresis loss).

Zheng *et al* reported the heat generation from various sizes of multilayer type piezoelectric ceramic actuators [30]. The temperature change was monitored in the actuators when driven at 3 kV mm^{-1} and 300 Hz , and figure 30 plots

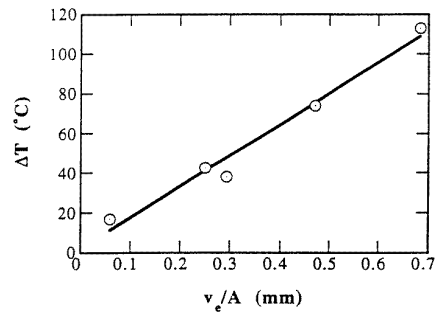


Figure 30. Temperature rise versus V_e/A (3 kV mm^{-1} , 300 Hz), where V_e is the effective volume generating the heat and A is the surface area dissipating the heat.

the saturated temperature as a function of V_e/A , where V_e is the effective volume (electrode overlapped part) and A is the surface area. This linear relation is reasonable because the volume V_e generates the heat and this heat is dissipated through the area A . Thus, if you need to suppress the heat, a small V_e/A design is preferred.

7.2. Frictional coating and lifetime

Figure 31 plots the efficiency and maximum output of various friction materials [31]. High ranking materials include PTFE (polytetrafluoroethylene, Teflon), PPS (Ryton), PBT (polybutyl terephthalate) and PEEK (polyethylethylketone). In practical motors, Econol (Sumitomo Chemical), carbon fiber reinforced plastic (Japan Carbon), PPS (Sumitomo Bakelite) and polyimide have been popularly used. Figure 32 shows the wear and driving period for CFRP, which indicates that the 0.5 mm thick coat corresponds to 6000 – 8000 hours life [32]. Although the lifetime of the ultrasonic motor is limited by the characteristics of the friction material, this problem has been nearly solved in practice for some cases. The durability test of the Shinsei motor (USR 30) is shown below:

continuous drive (CW 1 min and CCW 1 min) under revolution 250 rpm and load 0.5 kg cm

→ after 2000 hours, the revolution change is less than 10%

intermittent drive (CW 1 rotation and CCW 1 rotation) under no load

→ after 250 million revolutions, no degradation in motor characteristics.

Taking into account the usual lifetime specifications, e.g. 2000 – 3000 hours for VCRs, the lifetime of the ultrasonic motor is no longer a problem.

Of course, the lifetime of the motor itself is not identical to the lifetime installed in a device system. We need further clarification on this issue under severe drive conditions such as large load and high temperature and humidity.

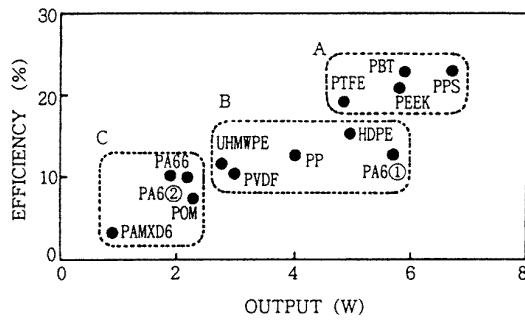


Figure 31. Efficiency and maximum output of the Shinsei ultrasonic motor for various friction materials.

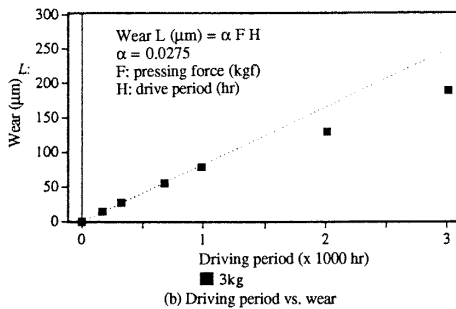
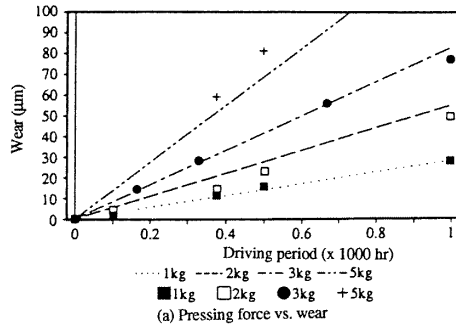


Figure 32. Wear and driving period of the ultrasonic motor for CFRP friction material.

7.3. Drive/control technique

Figure 33 summarizes the control methods of the ultrasonic motors. Taking account of the controllability and efficiency, pulse width modulation is most highly recommended.

Driving the motor at the antiresonant frequency, rather than at the resonant state, is also an intriguing technique to reduce the load on the piezo-ceramic and the power supply. Mechanical quality factor Q_m and temperature rise have been investigated on a PZT ceramic rectangular bar, and the results for the fundamental resonance (A-type) and antiresonance (B-type) modes are plotted in figure 34 as a function of vibration velocity [33]. It is recognized that Q_B is higher than Q_A over the whole vibration velocity range. In other words, the antiresonance mode can provide the same mechanical vibration level without generating heat. Moreover, the usage of ‘antiresonance’, whose admittance is very low, requires low current and high voltage for driving, in contrast to high current and low voltage for ‘resonance’. This means that a conventional inexpensive power supply may be utilized for driving the ultrasonic

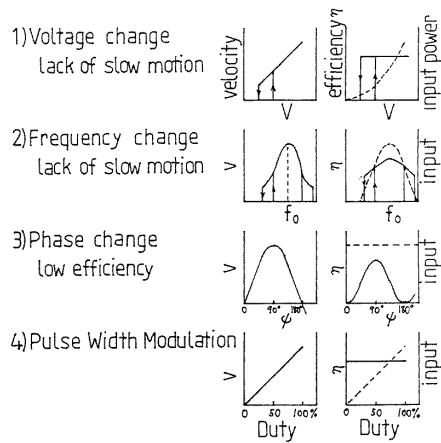


Figure 33. Control methods of the ultrasonic motors.

motor.

8. Summaries

8.1. Merits and demerits of ultrasonic motors

Ultrasonic motors are characterized by ‘low speed and high torque’, which are contrasted with ‘high speed and low torque’ of the conventional electromagnetic motors. Thus, the ultrasonic motors do not require gear mechanisms, leading to very quiet operation and space saving. Negligible effects from external magnetic or radioactive fields, and no generation of these fields are suitable for the application to electron beam lithography etc relevant to the semiconductor technology. Moreover, high power/weight ratio, high efficiency, compact size and light weight are very promising for the future micro-actuators adopted for catheter or tele-surgery.

8.2. Classifications of ultrasonic motors

There are various categories to classify ultrasonic motors such as:

- (1) operation: rotary type and linear type;
- (2) device geometry: rod type, π -shaped, ring (square) and cylinder types;
- (3) generating wave: standing wave type and propagating wave type.

8.3. Contact models for speed/thrust calculations

The following models have been proposed to calculate the speed/thrust of the ultrasonic motors:

- (1) rigid slider and rigid stator,
- (2) compliant slider and rigid stator,
- (3) compliant slider and compliant stator.

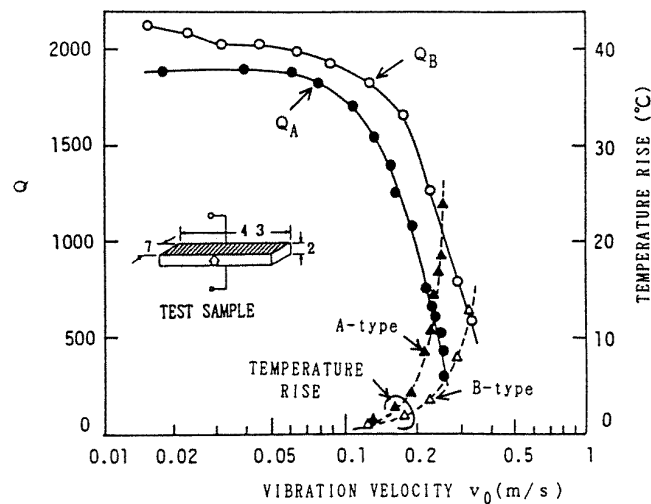


Figure 34. Vibration velocity dependence of the quality factor Q and temperature rise for both A (resonance) and B (antiresonance) type resonances of a longitudinally vibrating PZT rectangular transducer through d_{31} .

8.4. The ultrasonic motor development requirements

For the further applications of ultrasonic motors, systematic investigations on the following issues will be required:

- (1) low loss and high vibration velocity piezo-ceramics,
- (2) piezo-actuator designs with high resistance to fracture and good heat dissipation,
- (3) USM designs:
 - (a) displacement magnification mechanisms (horn, hinge-lever),
 - (b) USM types (standing-wave type, propagating-wave type),
 - (c) frictional contact part,
- (4) high frequency/high power supplies.

References

- [1] Barth H V 1973 *IBM Tech. Disclosure Bull.* **16** 2263
- [2] Lavrinenko V V, Vishnevski S S and Kartashev I K 1976 *Izv. Vyssh. Uchebn. Zaved. Radioelektron.* **13** 57
- [3] Vasiliev P E *et al* 1979 *UK Patent Application* GB 2020857 A
- [4] Sashida T 1982 *Oyo Butsuri* **51** 713
- [5] Kumada A 1985 *Japan. J. Appl. Phys.* **24** (Supplement 2) 739
- [6] Koc B 1998 *PhD Thesis* Electrical Engineering Department, The Pennsylvania State University
- [7] Fuda Y and Yoshida T 1994 *Ferroelectrics* **160** 323
- [8] Nakamura K, Kurosawa M and Ueha S 1993 *Proc. Japan. Acoust. Soc.* No 1-1-18, 917
- [9] Uchino K, Kato K and Tohda M 1988 *Ferroelectrics* **87** 331
- [10] Tomikawa Y, Nishituka T, Ogasawara T and Takano T 1989 *Sensors Mater.* **1** 359
- [11] Ueha S and Tomikawa Y 1993 *Ultrasonic Motors (Monographs in Electrical and Electronic Engineering 29)* (Oxford: Oxford Science)
- [12] 1983 *Nikkei Mech.* 28 Feb. 44
- [13] Kurosawa M, Ueha S and Mori E 1985 *J. Acoust. Soc. Am.* **77** 1431
- [14] Ueha S and Kuribayashi M 1986 *Ceramics* **21** 9
- [15] Sashida T 1983 *Mech. Automation Japan* **15** 31
- [16] Ise K 1987 *J. Acoust. Soc. Japan* **43** 184
- [17] Kasuga M, Satoh T, Tsukada N, Yamazaki T, Ogawa F, Suzuki M, Horikoshi I and Itoh T 1991 *J. Soc. Precision Eng.* **57** 63
- [18] Cummings J and Stutts D 1994 *Am. Ceram. Soc. Trans.* 147
- [19] Kumada A 1989 *Ultrason. Technol.* **1** 51
- [20] Tomikawa Y and Takano T 1990 *Nikkei Mech. Suppl.* 194
- [21] Yoshida T 1989 *Proc. 2nd Memorial Symp. on Solid Actuators of Japan: Ultra-precise Positioning Techniques and Solid Actuators for Them* p 1
- [22] Uchino K 1988 *Solid State Phys. Special Issue Ferroelectrics* **23** 632
- [23] Hayashi T 1984 *Proc. Japan. Electr. Commun. Soc. US84-8* 25
- [24] Ohnishi K, Naito K, Nakazawa T and Yamakoshi K 1991 *J. Acoust. Soc. Japan* **47** 27
- [25] Saigo H 1994 *15th Symp. on Ultrasonic Electronics, USE '94* PB-46 p 253
- [26] Takahashi M, Kurosawa M and Higuchi T 1994 *Proc. 6th Symp. on Electro-Magnetic Dynamics '94* 940-26 II, D718, p 349
- [27] Uchino K 1996 *Piezoelectric Actuators and Ultrasonic Motors* (Deventer: Kluwer)
- [28] Takahashi S and Hirose S 1993 *Japan. J. Appl. Phys.* **32** 2422
- [29] Hirose S, Aoyagi M, Tomikawa Y, Takahashi S and Uchino K 1995 *Proc. Ultrasonics Int. '95 (Edinburgh, 1995)* p 184
- [30] Zheng J, Takahashi S, Yoshikawa S, Uchino K and de Vries J W C 1996 *J. Am. Ceram. Soc.* **79** 3193
- [31] Tada Y, Ishikawa M and Sagara N 1991 *Polym. Preprints* **40** 1408
- [32] Ohnishi K *et al* 1993 *SAW Device 150 Committee, Japan. Acad. Promotion Inst., Abstract 36th Mtg* p 5
- [33] Hirose S, Takahashi S, Uchino K, Aoyagi M and Tomikawa Y 1995 *Mater. Res. Soc. Symp. Proc.* vol 360 (Pittsburgh, PA: Materials Research Society) p 15